COMMUNICATION

Reconfigurable T-junction DNA origami

Katherine G. Young,[a] Behnam Najafi,[a] William M. Sant,[b] Sonia Contera,[a] Ard A. Louis,[a] Jonathan P. K. Doye,[b] Andrew J. Turberfield[a] and Jonathan Bath*[a]

Abstract: DNA self-assembly allows the construction of nanometre-scale structures and devices. Structures with thousands of unique components are routinely assembled in good yield. Experimental progress has been rapid, based largely on empirical design rules. Here we demonstrate a DNA origami technique designed as a model system with which to explore the mechanism of assembly. The origami fold is controlled through single-stranded loops embedded in a double-stranded DNA template and is programmed by a set of double-stranded linkers that specify pairwise interactions between loop sequences. Assembly is via T-junctions formed by hybridization of single-stranded overhangs on the linkers with the loops. The sequence of loops on the template and the set of interaction rules embodied in the linkers can be reconfigured with ease. We show that a set of just two interaction rules can be used to assemble simple T-junction origami motifs and that assembly can be performed at room temperature.

DNA nanotechnology uses the information storage capacity of DNA to encode interactions between the component parts of nanometre-scale structures and devices. Simple rules based on Watson-Crick base pairing, and the geometry of double-stranded DNA, allow the construction of a diverse range of structures[1–5] at scale[6] and with an ever-increasing number of components.[7–9] This progress gives confidence that the technology will deliver useful applications.[10] Although assembly mechanisms have been studied theoretically[11–15] and experimentally[13, 16, 17], the assembly pathway is typically not considered during the design of DNA nanostructures. As the number of components increases it will become necessary to reuse components, for example by reusing the same folding motif within a structure. This constraint is relevant to folding of single-stranded RNA nanostructures where a limited number of motifs are available.[18, 19] The realization of biomimetic systems with multiple interacting components that are designed to assemble and operate in a crowded environment at a fixed temperature will require an understanding of assembly pathways and will likely involve design of marginally stable structures. With this in mind, we have designed a reconfigurable DNA origami system that will allow us to explore the relationship between sequence-programmed internal interactions and folded structure.

Here we use the T-junction to assemble DNA origami motifs. The T-junction is designed to join two double-stranded DNA molecules.[20] A short single-stranded domain at the end of one DNA duplex hybridizes to an internal loop in a second DNA duplex to form a characteristic T shape. Figure 1a shows a simple nanostructure comprising two T-junctions.

There are two variants of the T-junction: the 5' junction, formed by a 5' single-stranded overhang, is more stable than the 3' junction.[20] The 5' T-junction has been used to assemble 2D arrays,[20, 21] polyhedra,[21, 22] and RNA nanostructures.[23] It is well suited to systems designed for enzymatic[24] or enzyme-free[25, 26] copying. The weaker 3' T-junction has not been used as a construction motif although recent results suggest that both 5' and 3' motifs can be used.[27]

The template for T-junction origami is a double-stranded DNA containing a series of single-stranded loops. The template is assembled by annealing a long single strand with a complementary set of short oligonucleotides which contain the loop sequences and thus specify their positions on the template. The assembly of folded origami motifs is controlled by interaction between loops. Loop-loop interaction is mediated by double-stranded linkers with short single-stranded domains at either end which can form a T junction with complementary template loops. The set of linkers embodies a set of pairwise interaction rules that specify interactions that are allowed in the assembled origami motif.

We first characterize a simple U-shaped motif and observe cooperative assembly (Fig. 1). The template is a double-stranded molecule that contains four loops separated alternately by duplexes of 1.5 and 2 helical turns. The template is designed to form a U-shaped motif when mixed with the correct linker i.e. one that can bind to the first loop with its 5' end and the last loop with its 3' end (Fig. 1a). The set of linkers L_{10}, L_{01}, L_{11} and L_{00} were mixed with the template and the resulting complexes were resolved on a polyacrylamide gel (subscripts 1 and 0 indicate overhangs that are complementary and non-complementary to the corresponding loops: for example, the linker L_{10} contains a complementary domain at the 5' end and a non-complementary domain at the 3' end). L_{11} forms a slowly migrating complex consistent with assembly of the U-shaped motif containing both a 5' and a 3' T-junction (Fig. 1b, lane 5). L_{10} forms a complex with intermediate mobility, consistent with formation of the stronger 5' T-junction only (Fig. 1b, lane 4). L_{01} does not form a stable complex (Fig. 1b, lane 3): formation of a stable 3' T-junction is only observed in the presence of a 5' T-junction, i.e. as a result of cooperative assembly.

[a] Dr. K.G. Young, B. Najafi, Prof. S. Contera, Prof. A. A. Louis, Prof. A. J. Turberfield and Dr. J. Bath
Department of Physics
University of Oxford
Parks Road, Oxford OX1 3PU, UK
E-mail: j.bath@physics.ox.ac.uk
[b] W. M. Sant and Prof. J. P. Doye
Department of Chemistry
University of Oxford
South Parks Road, Oxford, OX1 3QZ, UK

Supporting information for this article is given via a link at the end of the document.

We use oxDNA,[28] a coarse-grained model of DNA, to simulate the formation of small T-junction motifs. The model reproduces the structural, mechanical, and thermodynamic properties of single- and double-stranded DNA and has been used to study many DNA nanostructures and devices.[15, 29, 30] It is well suited to the study of T-junction formation because it includes a natural description of the coaxial base stacking that stabilizes the ends of the linker. The model has recently been adapted to reproduce the difference between major and minor groove widths in duplex B-DNA:[31] this is important because the side branches of 5' and 3' T junctions span the major and minor groove respectively.[20]

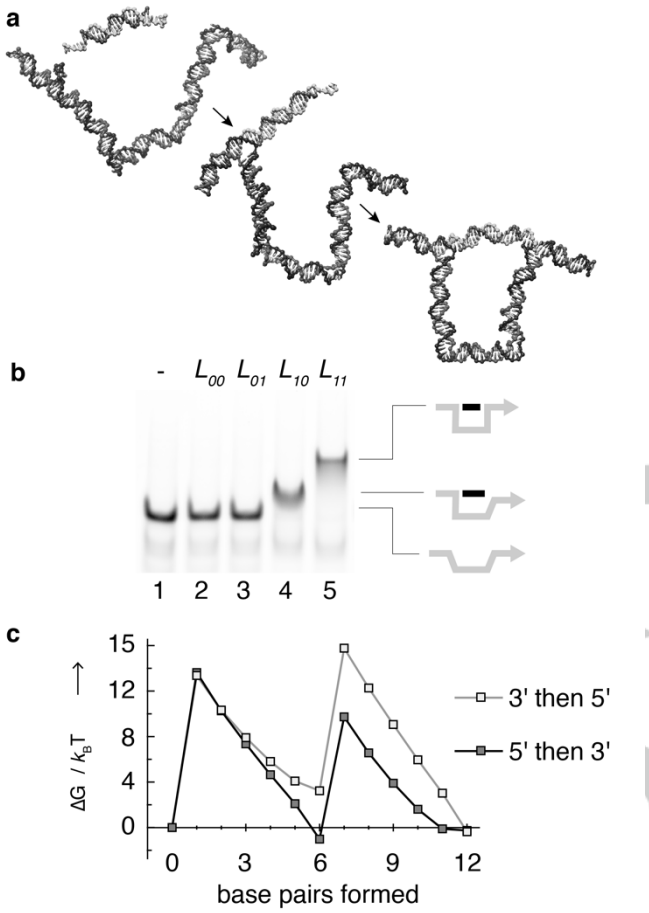

Figure 1. Cooperative binding of 5' and 3' T-junctions. **a** The template is designed to form a U-shaped structure comprising one 5' T-junction and one 3' T-junction when mixed with a double-stranded linker with complementary 5' and 3' overhangs at either end. **b** TAMRA-labelled template (100 nM) was mixed with linkers (150 nM) and run on an 8% polyacrylamide TAE gel containing 12.5 mM $MgCl_2$. The linkers are described using a subscript to denote complementary and non-complementary domains: for example, linker L_{10} has a domain complementary to a template loop at the 5' end but a dummy linker at the 3' end. **c** Free-energy landscape for formation of the U-shaped motif derived from oxDNA simulations at 25°C with all strands at 12.5 μM. The assembly temperature is above the melting point of the 3' T-junction in isolation but the two junctions can form cooperatively.

We consider two assembly pathways in which either the 5' T-junction or the 3' T-junction forms first. The free-energy landscapes of the two pathways were explored using umbrella sampling[32] (Fig. 1c). When the stronger 5' T-junction binds first, the local concentration at the corresponding loop of the 3' linker is increased, reducing the entropic barrier to formation of the 3' T-junction and thus stabilizing it. The simulation results corroborate the experimental observation that the two ends of the linker bind cooperatively.

To demonstrate the flexibility in design afforded by the T-junction origami, we next design two simple T-junction origami motifs, an extended motif and a compact motif (Fig. 2).

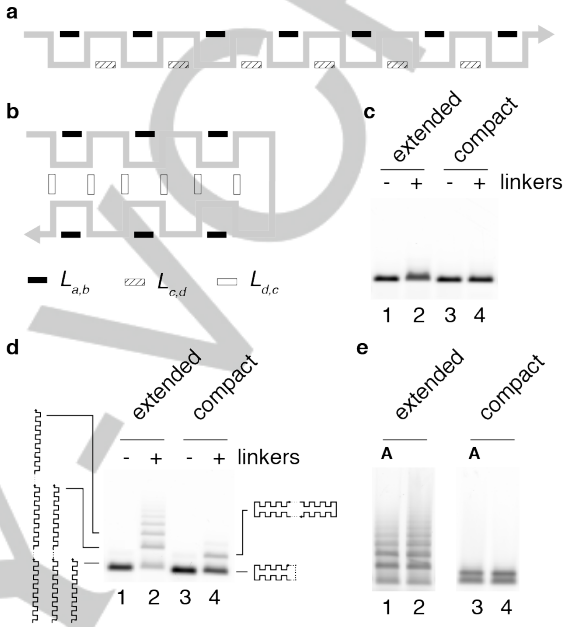

Figure 2. Two simple T-junction origami motifs: **a** The extended motif, and **b** the compact motif. Folding of the extended motif requires the linkers $L_{a,b}$ and $L_{c,d}$. To fold the compact motif the linker $L_{c,d}$ is replaced with the linker $L_{d,c}$. **c** Template and linkers were annealed and the resulting complexes were analysed in 0.7% agarose gels in TAE supplemented with 12.5 mM $MgCl_2$. **d** Hybridization of complementary tails, added to the 5' and 3' ends of the template, generates patterns of bands consistent with head-to-tail multimerization of the extended motif and head-to-head dimerization of the compact motif. **e** Similar patterns of bands are observed regardless of whether the template is annealed in the presence of the linkers (lanes 1 and 3, marked **A**) or incubated with linkers at room temperature (lanes 2 and 4).

Both designs use the same template incorporating 4 loop sequences [*a,b,c,d*]. They differ only in the linkers: [$L_{a,b}$, $L_{c,d}$] for the extended motif and [$L_{a,b}$, $L_{d,c}$] for the compact motif ($L_{n,m}$ indicates a linker with the complement of loop sequence *n* at the 5' end and the complement of loop sequence *m* at the 3' end). A single-stranded scaffold of 537 nt was generated by lambda exonuclease digestion of a PCR product amplified with a 5'-OH forward primer and a 5'-phosphate reverse primer.[33] The double-stranded T-junction origami template was made with a set of complementary strands, each with a single loop sequence inserted. The extended template comprises seven repeats of the sequence of loops *a,c,d,b*. Adjacent loops are spaced alternately at 1.5 and 2 turn intervals. The only difference between the templates for the extended and compact origami motifs is that at the centre of the compact template two loop strands are replaced with a single splint strand without loops in order to produce a rigid spacer.

Assembly of the extended and compact motifs was assessed by annealing the scaffold and loop strands in the presence or

absence of linker strands and analysing the products on agarose gels. Structures formed in the presence of the linkers have approximately the same electrophoretic mobility as the template alone (Fig. 2c). If correctly assembled, the extended and compact motifs differ in the disposition of the two ends of the template: the ends of the extended motif are at opposite sides of the structure separated by ~150 nm whereas the ends of the compact structure are held close together. We reasoned that if complementary single-stranded tails are added to opposite ends of the template then copies of the extended motif will join head-to-tail to from linear chains whereas copies of the compact motif will join head-to-head to form cyclic dimers. As anticipated, the extended motif with complementary tails at either end of the template produces a ladder of bands (Fig. 2d, lane 2) whereas the compact motif produces a mixture of monomer and dimer which we assume to be head-to-head (Fig. 2d, lane 4). The pattern of bands observed when all components are annealed is consistent with correct assembly of both the extended and the compact motifs. The same pattern of bands is observed when linkers are mixed with the double-stranded template and incubated at room temperature, consistent with isothermal assembly of T-junction origami.

Structures annealed in the presence of the linkers were purified from agarose gels and imaged using AFM. The T-junction origami structures proved to be harder to image than a standard DNA origami, perhaps because they are less structurally stable. Both the extended motif (Fig. 3) and the compact motif (Fig. 4) fold to give the predicted shapes. In both cases the yield of well-folded structures is low. Misfolded extended motifs typically have a characteristic zig-zag shape (Fig. 3c) which we attribute to half-bound linkers. Given that the 5' T-junction is more stable than the 3' motif it is likely that the half-bound linkers are bound at the 5' end only.

The compact motif shows a more heterogenous distribution of folds (Fig. 4). Well-folded structures are observed (Fig. 4b) but they are relatively scarce. In a common type of mis-fold, elements that are designed to lie opposite each other in the well-folded structure have slipped out of register (compare Fig. 4b and Fig. 4c).

Unlike a traditional DNA origami, the two T-junction origami motifs contain repeated components and as a result there is significant potential for misfolding. The extended motif has 7 copies of the linker $L_{a,b}$ and 6 copies of the linker $L_{c,d}$; the compact motif has 6 copies each of linkers $L_{a,b}$ and $L_{d,c}$. Ignoring any steric constraints there are more than 5×10^5 misfolded configurations available (6! × 6!). The folding yield is much higher than would be expected from random sampling of the available configurations.[13]

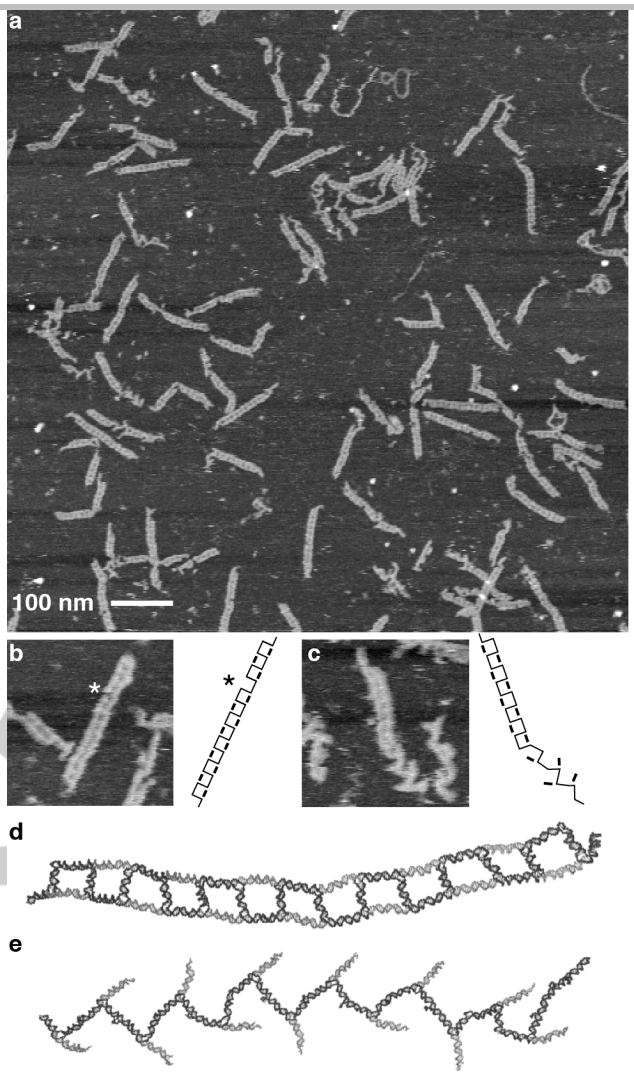

Figure 3. AFM of the extended motif. **a** 1 μm field of view. **b** Well-folded structure perhaps missing a single linker (marked with an asterisk). **c** Part-folded structure with some linkers bound by the 5' end only. **d** oxDNA model for the folded extended structure. **e** oxDNA model for an extended structure unfolded by pulling.

The extended motif folds in higher yield than the compact motif. Interactions that stabilize the extended motif are short-range compared to those that stabilize the compact motif (the extended motif has a contact order[34] of 0.1, the compact motif has a contact order of 0.24: these values fall either side of the values reported for protein folds[34]). It is therefore reasonable to expect that the extended motif would fold faster than the compact motif. However, folding of the compact motif is likely to be more cooperative: when a linker binds and brings two distant segments of the template into close proximity, binding of an adjacent linker is greatly enhanced.

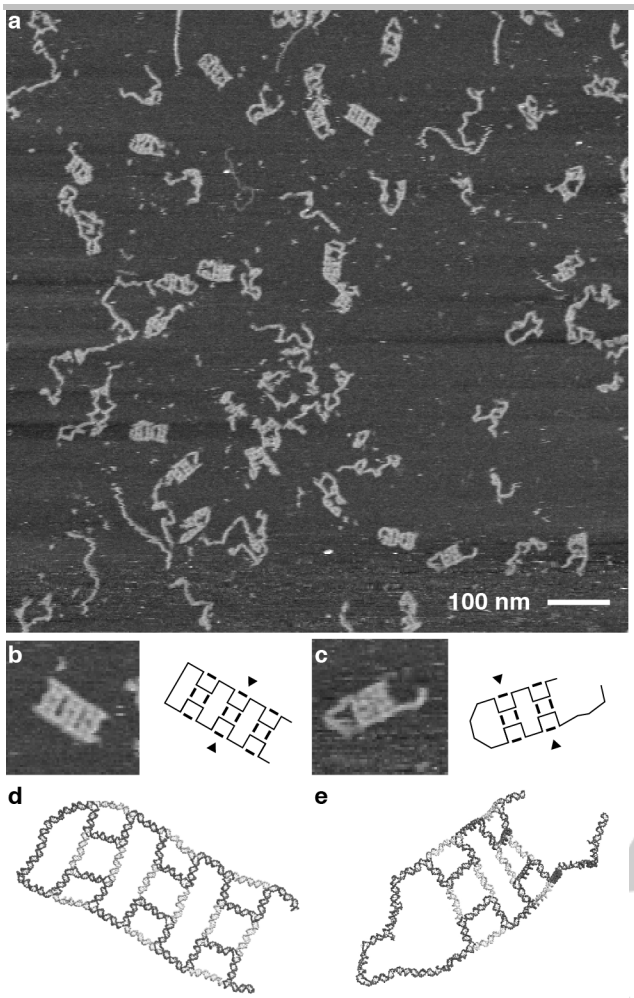

Figure 4. AFM of the compact motif. **a** 1 μm field of view. **b** Well-folded structure. **c** Misfolded structure where elements that are aligned in the well-folded structure (marked with triangles) have slipped in the misfolded structure. **d** oxDNA model for the compact motif. **e** oxDNA model for the misfolded compact motif.

imaging force for tapping mode AFM under the conditions used here is ~100 pN, although the lateral force is considerably less.

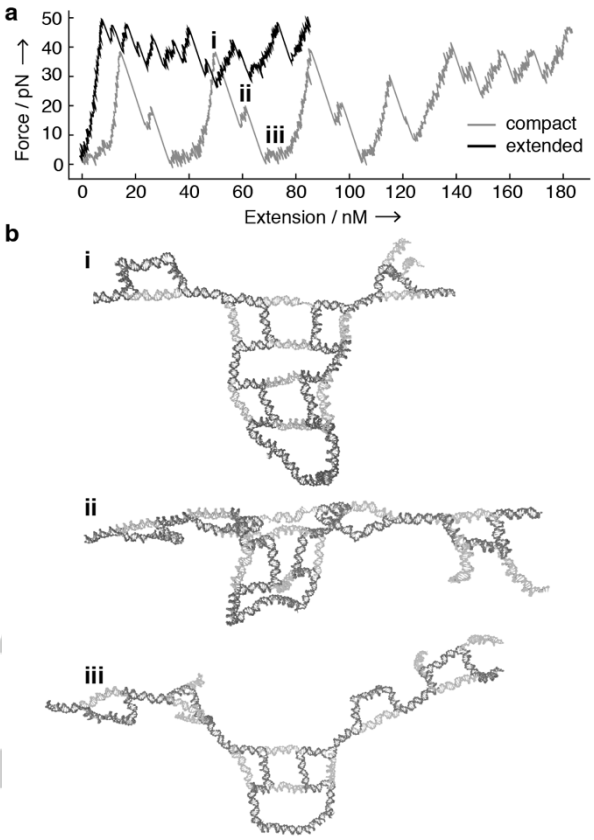

Figure 5. oxDNA unfolding simulations. **a** Force-extension curves for unfolding of the extended and compact motifs at a force loading rate of 3.2 x 10^6 pN s^{-1} and a temperature of 25°C. **b** Examples of unfolding intermediates of the compact motif corresponding to annotated regions (**i**, **ii**, **iii**) of the force-extension curve. Unfolding intermediates of the extended motif are shown in the Supporting Information.

To assess the potential sensitivity of the two T-junction origami to damage by the forces exerted by the AFM, we used oxDNA to examine the force-induced unravelling of the two origamis when subject to tensile forces at either end. Although the method of force application is different from the lateral forces applied by an AFM tip, the results should be indicative of the robustness of the origami to mechanical probing. The force-extension curves for the two origamis are illustrated in Fig. 5a for the slowest force loading rate simulated. As the rate is still faster than typical in experiment, the rupture forces should be seen as upper bounds to those that might apply on experimental time scales. (Fig. S2 illustrates the decrease in the rupture forces as the pulling rate is decreased.)

Each force-extension curve has a sawtooth structure with each force drop associated with the dissociation of one end of a single linker (or occasionally two linkers); the final states are similar to that shown in Fig. 3e where the linkers are all attached to the scaffold by one end (complete dissociation of the linkers occurs only at higher forces). For the extended motif, the rupture forces are typically between 30 pN and 50 pN, whereas for the compact motif they are lower, always below 40 pN, suggesting that this motif has a greater susceptibility to AFM damage. The

Lower rupture forces are observed for the compact motif because tensile forces are more concentrated along single linkers. It unravels initially by sequential breaking of the long-range links connecting the two halves of the motif, starting with the linkers closest to the ends. Each of these ruptures leads to a large increase in end-to-end distance and therefore a large drop in force. There is a thrice-repeated pattern in the force-extension curves associated with the breaking of the three pairs of these long-range links: structures associated with breaking of the second pair are illustrated in Fig. 5b. This mechanical unfolding pathway is in some ways the reverse of the expected self-assembly pathway. The local linkages that are expected to form first break last, and the longer-range connections that are expected to form last and in order of increasing separation along the scaffold break first and in the opposite order.

We have shown that 5' T-junctions and the weaker 3' T-junctions can be combined to make a foldable polymer DNA nanostructure. The fraction of fully-formed structures imaged by AFM is low, perhaps because the structures are more susceptible to damage during AFM imaging than traditional DNA origami. More robust structures could be designed using only 5' T-

junctions (for example by moving some loop sequences from the top strand of the template to the bottom strand). T-junction DNA origami motifs have properties that are quite different from those of traditional DNA origami structures because they are formed by relatively weak interactions.

T-junction DNA origami is a useful system with which to explore self-assembly of foldable polymers because of the ease with which it can be reconfigured. The sequence of loops on the template can be changed by substituting the loop-containing oligonucleotides. An interaction rule can be changed by substituting one linker for another. Competitive interactions can be explored by adding competing linkers. Interaction strengths can be modified by changing linker concentrations or loop sequences. We anticipate that it will be possible to generate larger structures by using simple motifs such as the ones demonstrated here as building blocks.

Experimental Section

DNA nucleotide sequences, experimental methods and simulation methods[35] are described in the Supporting Information.

Acknowledgements

KGY was supported by EPSRC & BBSRC Life Sciences Interface DTC (EP/F500394/1) and AJT by a Royal Society Wolfson Research Merit Award.

Keywords: DNA origami • T-junction • self-assembly • DNA nanotechnology

1 E. Winfree, F. Liu, L. A. Wenzler, N. C. Seeman *Nature* **1998**, *394*, 539-544

2 W. M. Shih, J. D. Quispe, G. F. Joyce, *Nature* **2004**, *427*, 618-621.

3 P. W. K. Rothemund, *Nature* **2006**, *440*, 297-302.

4 S. M. Douglas, H. Dietz, T. Liedl, B. Högberg, F. Graf, W. M. Shih, *Nature* **2009**, *459*, 414-418.

5 E. Benson, A. Mohammed, J. Gardell, S. Masich, E. Czeizler, P. Orponen, B. Högberg, *Nature* **2015**, *523*, 441-444.

6 F. Praetorius, B. Kick, K. L. Behler, M. N. Honemann, D. Weuster-Botz, H. Dietz, *Nature* **2017** *552*, 84–87.

7 K. F. Wagenbauer, C. Sigl, H. Dietz, *Nature* **2017**, *552*, 78–83.

8 G. Tikhomirov, P. Petersen, L. Qian, *Nature* **2017**, *552*, 67–71.

9 L. L. Ong, N. Hanikel, O. K. Yaghi, C. Grun, M. T. Strauss, P. Bron, J. Lai-Kee-Him, F. Schueder, B. Wang, P. Wang, J. Y. Kishi, C. Myhrvold, A. Zhu, R. Jungmann, G. Bellot, Y. Ke, P. Yin, *Nature* **2017**, *552*, 72-77.

10 a) K. Sanderson, *Nature* **2010**, *464*, 158-159. b) *Nature* **2016**, *531*, 276.

11 W. M. Jacobs, D. Frenkel, *J. Am. Chem. Soc.* **2016**, *138*, 2457-2467.

12 M. Sajfutdinow, W. M. Jacobs, A. Reinhardt, C. Schneider, D. M. Smith, *Proc. Natl. Acad. Sci. USA* **2018**, *115*, E5877-E5886.

13 K. E. Dunn, F. Dannenberg, T. E. Ouldridge, M. Kwiatkowska, A. J. Turberfield, J. Bath, *Nature* **2015**, *525*, 82-86.

14 A. Cumberworth, A, Reinhardt, D. Frenkel, *J. Chem. Phys.* **2018**, *149*, 234905.

15 B.E. K. Snodin, F. Romano, L. Rovigatti, T. E. Ouldridge, A. A. Louis and J. P. K. Doye, *ACS Nano*, **2016**, *10*, 1724-1737.

16 J. M. Majikes, J. A. Nash, T. H. LaBean, *New J. Phys.* **2016**, *18*, 115001.

17 F. Schneider, N. Móritz and H. Dietz, *Science Advances*, **2019**, *5*, eaaw1423.

18 L. Jaeger, A. Chworos, *Curr. Opin. Struct. Biol.* **2006**, *16*, 531-543.

19 C. Geary, P. W. K. Rothemund, E. S. Andersen, *Science* **2014**, *345*, 799-804.

20 S. Hamada, S. Murata, *Angew. Chem.* **2009**, *118*, 1-5; *Angew. Chem. Int. Ed.* **2009**, *121*, 6592-6955.

21 M. Li, H. Zuo, J. Yu, X. Zhao, C. Mao, *Nanoscale*, **2017**, *9*, 10610-10605.

22 X. Li, C. Zhang, C. Hao, C. Tian, G. Wang, C. Mao, *ACS Nano*, 2012, *6*, 5138-5142.

23 J. Yu, Z. Liu, W. Jiang, G. Wang, C. Mao, *Nat. Comm.* **2015**, *6*, 5724.

24 R. Kageyama, I. Kawamata, K. Tanabe, Y. Suzuki, S. Nomura, S. Murata. *ChemBioChem*, **2018**, *19*, 873-876.

25 H. Chandran, N. Gopalkrishnan, B. Yurke, J. Reif, *J. R. Soc. Interface* **2012**, *9*, 1637-1652.

26 J. Kim, J. Lee, S. Hamada, S. Murata & S.H. Park, *Nat. Nanotech.* **2015**, *10*, 528-533.

27 B. Najafi, K. G. Young, J. Bath, A. A. Louis, J. P. K. Doye and A. J. Turberfield, arXiv:2005.11545.

28 T. E. Ouldridge, A. A. Louis and J. P. K. Doye, *J. Chem. Phys.* .**2011**, *134*, 085101.

29 N. Srinivas. T. E. Ouldridge, P. Šulc, J. M. Schaeffer, B. Yurke, A. A. Louis, J. P. K. Doye, E. Winfree, *Nucleic Acids Res.* **2013**, *41*, 10641-10658.

30 T. E. Ouldridge, R. H. Hoare, A. A. Louis, J. P. K. Doye, J. Bath, A. J. Turberfield, *ACS Nano*, **2013**, *73*, 2479-2490.

31 B. E. K. Snodin, F. Randisi, M. Mosayebi, P. Šulc, J. S.Schreck, F. Romano, T. E. Ouldridge, R. Tsukanov, E. Nir, A. A. Louis and J. P. K. Doye, *J. Chem. Phys.* **2015**, *142*, 234901.

32 G. Torrie and J. Valleau, J. Comput. Phys. **1977**, 23, 187-199.

33 A. J. H. Smith, Nucleic Acids Res.**1979,** *6*, 831-848.

34 K. W. Plaxco, K. T. Simons and D. Baker, *J. Mol. Biol.*, **1998**, *277*, 485-494.

35 a) S. Whitelam, E. H. Feng, M. F. Hagan, P. L. Geissler, *Soft Matter,* **2008**, *5*, 1251-1262 b) S. Kumar, J. M. Rosenberg, D. Bouzida, R. H. Swendsen and P. A. Kollman, *J. Comp. Chem.* **1992**, *13*, 1011-1021. c) J. Russo, P. Tartaglia and F. Sciortino, *J. Chem, Phys.* **2009**, *131*, 014504. d) M. C. Engel, D. M. Smith, M. A. Jobst, M. Sajfutdinow, T. Liedl, F. Romano, L. Rovigatti, A. A. Louis and J. P. K. Doye, *ACS Nano*, **2018**, *12*, 6734-6747.

COMMUNICATION

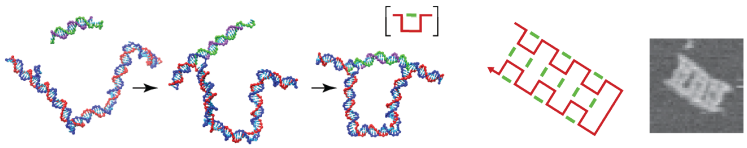

*Katherine G. Young, Behnam Najafi, Willam M. Sant, Sonia Contera, Ard A. Louis, Jonathan P. K. Doye, Andrew J. Turberfield and Jonathan Bath**

Page No. – Page No.

A foldable polymer DNA origami assembled using T-junction motifs.